1028

Université de Neuchâtel
Faculté des Sciences

Etude de l'induction asymétrique lors de la réaction de transfert d'électrons entre des complexes de symétrie C_2 du cobalt (III) et du fer (II)

Forme réduite de la thèse présentée à la Faculté des Sciences par :

PHILIPPE POUSAZ

Ingénieur chimiste diplômé de l'Université de Neuchâtel pour l'obtention du grade de Docteur ès sciences

Institut de Chimie
de l'Université de
Neuchâtel

Novembre 1982

IMPRIMATUR POUR LA THÈSE

Etude de l'induction asymétrique lors de la réaction de transfert d'électron entre des complexes de symétrie C_2 du cobalt(III) et du fer(II)

de M*onsieur Philippe Pousaz*

UNIVERSITÉ DE NEUCHATEL

FACULTÉ DES SCIENCES

La Faculté des sciences de l'Université de Neuchâtel, sur le rapport des membres du jury,

M. K. Bernauer, Mme E. Stoeckli-Evans et M. S. Fallab (Bâle)

autorise l'impression de la présente thèse.

Neuchâtel, le *5 juin 1984*

Le doyen:

H. Beck

H. Beck

Separatum
HELVETICA CHIMICA ACTA
Volumen 67, Fasciculus tertius (1984)

90. Stereoselectivity in Reactions of Metal Complexes IX[1])

Stereoselective Formation of Cobalt(III) Complexes with New Linear Pentadentate Ligands

by **Klaus Bernauer*** and **Philippe Pousaz**[2])

Laboratoire de Chimie Inorganique et Analytique de l'Université de Neuchâtel, Bellevaux 51, CH-2000 Neuchâtel

(21.II.84)

Summary

The synthesis of cobalt(III) complexes with the new linear pentadentate ligands meso- and racemic 2,6-bis(3-carboxy-1,2-dimethyl-2-azapropyl)pyridine (**1a** and **1b**), respectively, and 2,6-bis[(3*S*)-3-carboxy-4-methyl-2-azapentyl]pyridine (**2**) are described. Only one of the different possible isomers is obtained from each ligand. The structure of the complexes has been assigned on the basis of their ^{1}H-NMR and CD spectra. The structure of the aqua-cobalt(III)-**1a** and the aqua-cobalt(III)-**1b** has been confirmed by X-ray analysis. Partial resolution of optical antipodes of the aqua-cobalt(III)-**1b** was achieved by column chromatography and a tentative assignment of their absolute configuration is made.

Introduction. – Multidentate ligands react frequently with metal ions by the formation of several geometrical isomers. By the introduction of special structural features in the framework of these ligands, certain of these isomers may be favored or even formed exclusively. Reactions with these ligands are then called stereospecific. When the selection occurs between diastereoisomers, the reaction is called diastereoselective. The knowledge of the factors leading to diastereoselectivity are of special interest in order to perform asymmetric reactions.

Between the great number of ligands reacting in a diastereoselective way, linear pentadentate ligands are not very frequent, but have the advantage of leaving only one coordination site free in an octahedral coordination sphere. Therefore, such ligands may be particularly appropriate for the study of the stereoselectivity of inner sphere electron transfer reactions. Some results in this field will be presented in a following paper.

Four geometrical isomers may be formed with a linear pentadentate ligand, three of them existing as optical antipodes [2].

---

[1]) Part VIII, see [1].

[2]) Part of Ph. D. thesis of *Ph. P.*, Université de Neuchâtel.

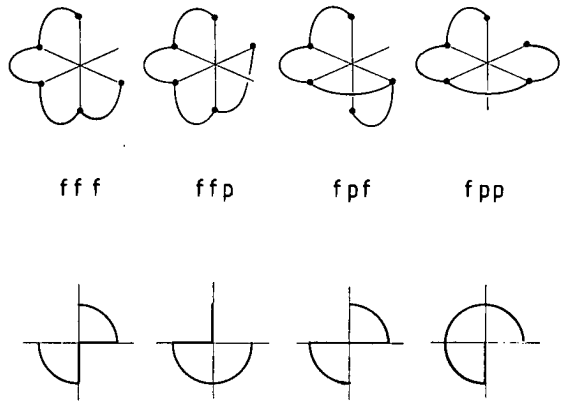

Fig. 1. *Geometrical isomers of octahedral complexes formed with linear pentadentate ligands*

The four isomers are characterized by the facial (f) or peripheric (p) arrangement of the three pairs of adjacent chelate rings and show a typical pattern, when the observer is looking towards the metal ion from the free coordination site *(Fig. 1)*.

For reasons presented in [3] we have choosen the (fpf) arrangement showing C_2-symmetry for the present study of stereoselective formation of inert octahedral cobalt(III) complexes.

To ensure the selection of the basic (fpf) geometry, a central pyridine unity substituted in the 2,6-positions is used. Such an arrangement must coordinate in a peripheric way for obvious steric reasons. On the other hand, the facial coordination of lateral chelate rings is strongly favored by the presence of a saturated N-atom as the coordinating atom connecting two five-membered chelate rings. It is well-known that a peripheric arrangement of such groups is strained and is only found in cases where the facial arrangement is not possible [4]. The chirality of the complex can now be fixed by the introduction of substituents into the ligand and by choosing a given chirality of the asymmetric C-atoms. These asymmetric centers should then fix the absolute configuration of the two tetrahedrally coordinated N-atoms. The substituents may be introduced either into the chelate rings formed by the pyridine unity and the tetrahedral N-atoms (type **I**) or into the chelate rings formed by the amino-carboxylate groups (type **II**).

Scheme

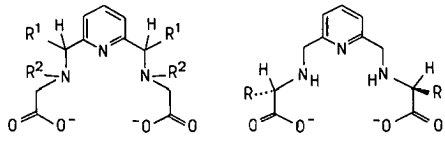

type I type II

1 $R^1 = R^2 = CH_3$ **2** $R = CH(CH_3)_2$
1a (1*R*,1′*S*) = *meso*-form
1b (1*RS*,1′*RS*) = racemic form

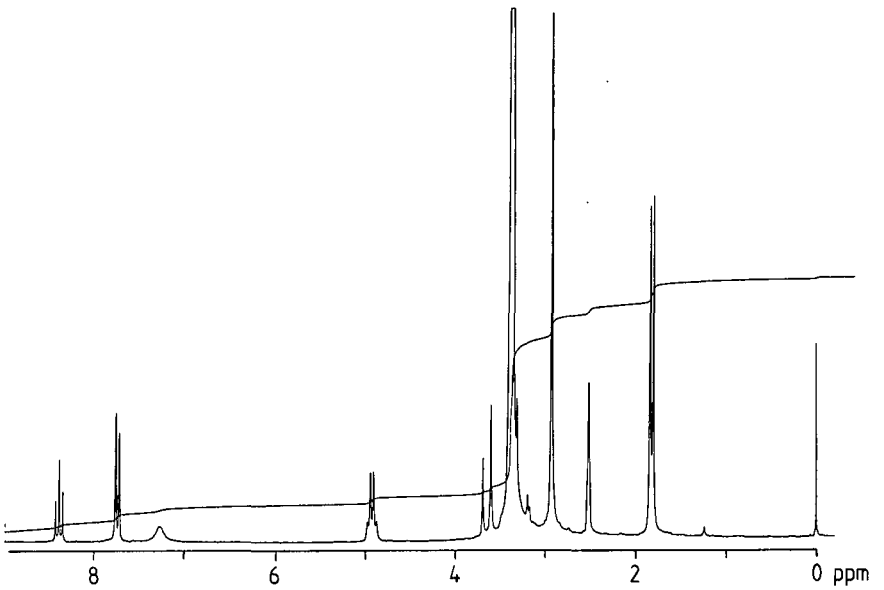

Fig. 2. *^{1}H-NMR Spectrum of aqua(2,6-bis[(1*RS,*1'*RS*)-3-carboxy-1,2-dimethyl-2-azapropyl]pyridine)cobalt(III) hexafluorophosphate* (racemic complex; 200 MHz, DMSO)

Results and Discussion. – The pentadentate ligand 2,6-bis[3-carboxy-1,2-dimethyl-2-azapropyl]-pyridine (**1**) exists in a *meso*- (**1a**) and in a racemic form (**1b**). Attempts to separate the two isomers of the free ligand failed. However, when the cationic aqua-cobalt(III) complex of the ligand mixture was crystallized as hexafluorophosphate (or as perchlorate), two clearly distinct crystalline forms were obtained; one consists of fine red needles and contains the racemic form of the ligand; the other is obtained as dark red plates and represents the complex containing the *meso*-form of the ligand. The two complexes were identified by their ^{1}H-NMR spectrum, represented in *Fig. 2* for the racemic and in *Fig. 3* for the *meso*-form.

As seen in these spectra, almost all the signals are doubled in the *meso*-form due to a different arrangement of the two halves of the ligand molecule in the complex, whereas the racemic form shows two identical halves, indicating perfect C_2-symmetry in the ligand arrangement.

The conclusions drawn from the ^{1}H-NMR spectra were finally confirmed by an X-ray structural analysis of the two solids; their molecular structure is shown in *Fig. 4* [5].

From these results it follows that in all the cases of complexes with this type of ligand, the basic geometry is the same, independent of the steric influences of the substituents. Any isomer showing the two carboxylate groups in *cis*-position (fpp structure; *cf. Fig. 1*) can be excluded. In the complex formed by the *meso*-ligand, the two lateral chelate rings are therefore not differentiated by their relative geometrical arrangement with respect to the rest of the molecule, but only by the relative position of the substituents on the two central chelate rings. In one of these the two neighbouring methyl groups are in an almost eclipsed conformation, whereas in the complex

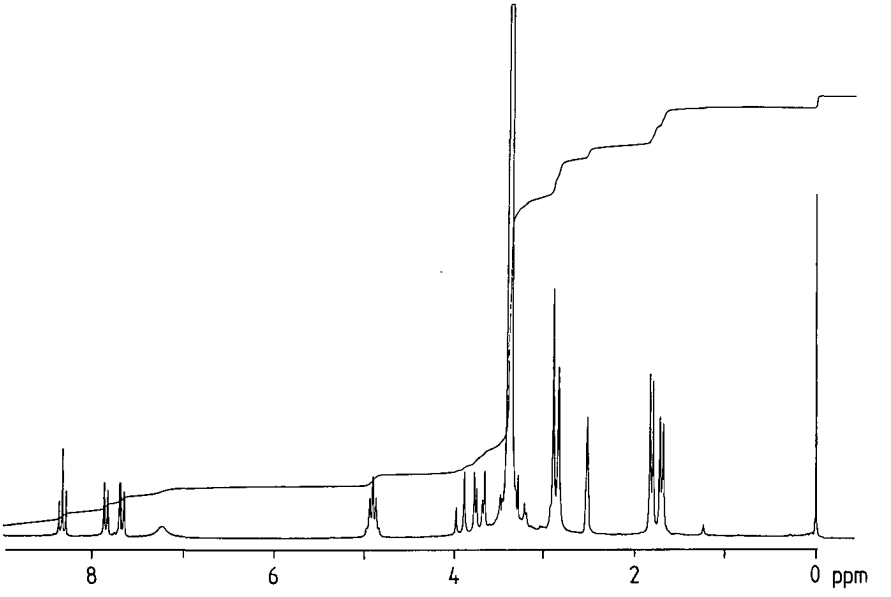

Fig. 3. *^{1}H-NMR Spectrum of the aqua(2,6-bis[(1*R,*1'*S*)-3-carboxy-1,2-dimethyl-2-azapropyl]pyridine)cobalt(III) hexafluorophosphate* (*meso*-complex; 200 MHz, DMSO)

with the racemic ligand both chelate rings have their substituents in the most stable staggered arrangement. The complex will therefore assume a configuration of predictable chirality, when the chirality of the asymmetric C-atoms is given.

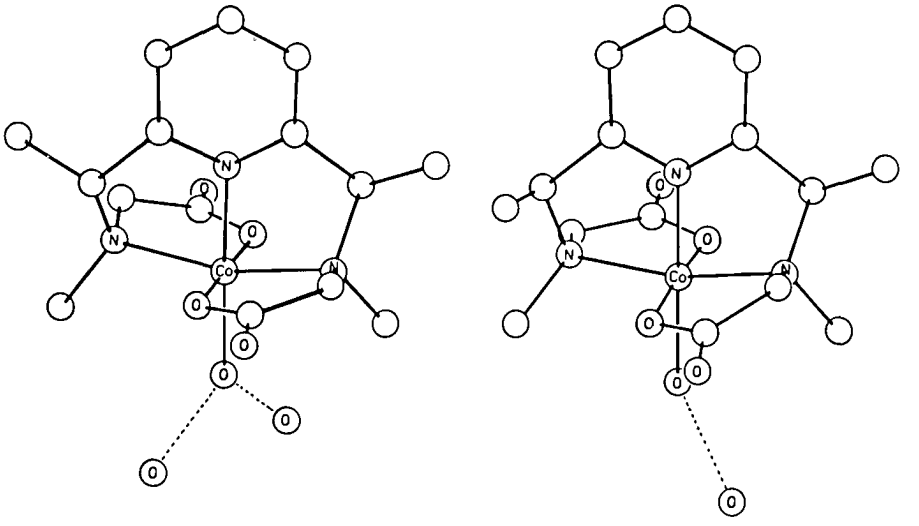

Fig. 4. *Molecular structures of the aqua(2,6-bis[(1*RS,*1'*RS*)-3-carboxy-1,2-dimethyl-2-azapropyl]pyridine)-cobalt(III) hexafluorophosphate* (**1b**, racemic complex) *and of the aqua(2,6-bis[(1*R,*1'*S*)-3-carboxy-1,2-dimethyl-2-azapropyl]pyridine)cobalt(III) hexafluorophosphate* (**1a**, *meso*-complex)

For the purpose of future studies, we were mainly interested by the complex containing the racemic ligand and the first problem which arose, was the separation of the complex into its optical antipodes. This separation could be achieved by elution chromatography of the complex using potassium antimonyltartrate as the optically active eluent, and by precipitation of the racemic perchlorate from the partially enriched fractions. *Fig. 5* shows the CD spectra of the solutions of fractions of the highest optical activity obtained. When these CD spectra are compared with the corresponding spectrum of the aqua-(2,6-bis[(3*S*)-3-carboxy-4-methyl-2-azapentyl]pyridine)cobalt(III) the absolute configuration *Λ*-aqua-(2,6-bis[(1*S*,1'*S*)-3-carboxy-1,2-dimethyl-2-azapropyl]pyridine)cobalt(III) may tentatively be attributed to the complex showing a negative CD band at 530 nm (curve *a*, *Fig. 5*).

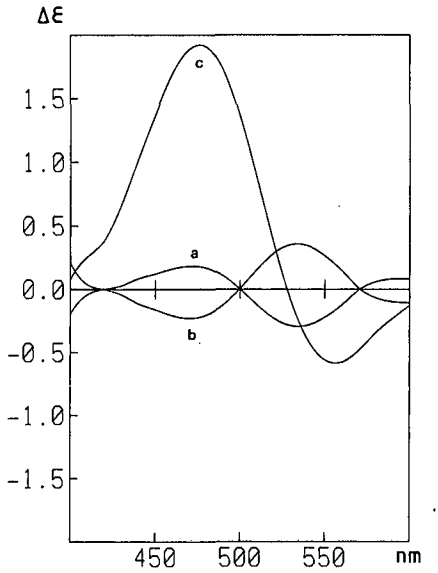

Fig. 5. *CD spectra of:* a) *Λ-aqua(2,6-bis[(1*S*,1'*S*)-3-carboxy-1,2-dimethyl-2-azapropyl]pyridine)cobalt(III) perchlorate,* b) *Δ-aqua(2,6-bis[(1*R*,1'*R*)-3-carboxy-1,2-dimethyl-2-azapropyl]pyridine)cobalt(III) perchlorate,* c) *Λ-aqua(2,6-bis[(3*S*)-3-carboxy-4-methyl-2-azapentyl]pyridine)cobalt(III) hexafluorophasphate.* Tentative attribution of the absolute configuration as discussed in the text.

As an example of ligands of type **II** we prepared the 2,6-bis[(3*S*)-3-carboxy-4-methyl-2-azapentyl]pyridine (**2**). The advantage of this type of ligand lies in the fact that only one isomer is obtained when an optically active amino acid is used as starting material. The cobalt(III) complex prepared from this ligand may exist in two diastereoisomeric forms. They are shown in *Fig. 6* for the ligand with the (*S,S*)-configuration.

A tentative assignment of the absolute configuration of the compound obtained may be based on ^{1}H-NMR spectra. It is known that in cobalt(III) complexes of ethylenediamine diacetic acid, $[Co^{III}(EDDA)(en)]^+$, the methylene group in the amino-acid moiety shows different chemical shifts for the H_a (*exo*) and H_b (*endo*) proton (the signal for H_a appears at lower field than that for H_b due to the magnetic anisotropy of

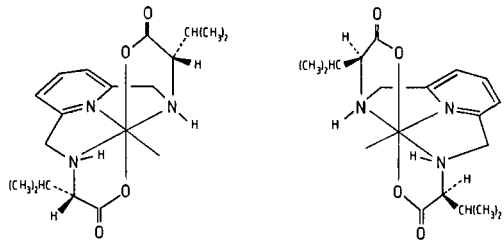

Fig. 6. *Possible diastereoisomeric forms of (2,6-bis[(3S)-3-carboxy-4-methyl-2-azapentyl]pyridine)cobalt(III) complex*

the C–N bond [6]). When one of the two types of protons is replaced by a substituent, the signal of the corresponding proton disappears, whereas the other remains almost unchanged. By this method *Cooke et al.* [6] attributed the absolute configuration of the $[Co^{III}(EDDP)(en)]^+$-isomers by comparison of their ^{1}H-NMR spectra with that of the $[Co^{III}(EDDA)(en)]^+$-complex. The partial spectrum (*1* of *Fig. 7*) shows the H_a-proton (3.6 ppm) and H_b-proton (3.3. ppm) of our aqua-cobalt(III)-**1b** complex; the spectrum (*2* of *Fig. 7*) corresponding to the aqua-cobalt(III)-**2** complex, exhibits only an H_b (3.2 ppm) proton signal indicating that the isopropyl group has replaced the H_a-proton. Therefore the cobalt(III)-**2** complex should have the *Λ-exo*-configuration when the ligand is obtained from the (*S*)-amino acid.

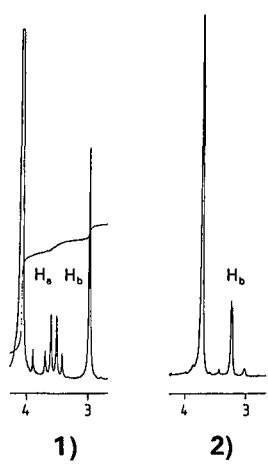

Fig. 7. *Partial ^{1}H-NMR spectra of:* 1) *aqua-cobalt(III)-***1b** *complex* (DMSO, 200 MHz) *after addition of D_2SO_4 in order to shift the water signal,* 2) *aqua-cobalt(III)-***2** *complex* (DMSO, 200 MHz)

We are grateful to Dr. *H. Stoeckli* and Dr. *L. Brehm* for the X-ray analyses, to Dr. *S. Claude* for the NMR spectra and to Dr. *G. Jeanneret* for his assistance in synthetic work.

Experimental Part

1. *General.* Optical rotations were measured on a *Perkin-Elmer 241* polarimeter, UV and VIS spectra were measured on a *Uvikon 820* spectrophotometer and CD measurements were obtained from a *Jasco J-500* spectropolarimeter. ^{1}H-NMR spectra were recorded on a *Bruker WP200* at 200 MHz and on a *Hitachi Perkin-Elmer R24B* at 60 MHz.

2. *Syntheses.* – 2.1. *2,6-bis[1-(*N*-methylamino)ethyl)]pyridine* [7]. 2,6-Bis(acetyl)pyridine (25 g, 0.15 mol) [8] was added to 750 ml of an ethanolic solution of 33% CH_3NH_2. The mixture was hydrogenated for 10 h at r.t. and 4 atm. in the presence of Pt/C (10%) as catalyst. The solution was filtered on *Celite* and EtOH and excess CH_3NH_2 were evaporated under vacuum. The residual yellowish oil was distilled at 0.15 mm/Hg and the main fraction (b.p. 78–79°) collected. Yield: 18 g (60%). ^{1}H-NMR (200 MHz; $CDCl_3$): 1.7 (*d*, *J* = 7.5, 6H); 2.6 (*s*, 2H); 4.1 (*q*, *J* = 7.5, 2H); 7.5 (*d*, *J* = 7.5, 2H); 8.0 (*t*, *J* = 7.5, 1H).

The product, which constitues a mixture of the *meso*- and racemic form was used for synthesis without further purification.

2.2. *2,6-Bis(3-carboxy-1,2-dimethyl-2-azapropyl)pyridine.* A concentrated aq. solution of 10.28 g (0.11 mol) of chloroacetic acid was added slowly to a solution of 10 g (0.05 mol) of 2,6-bis[1-(*N*-methylamino)ethyl]pyridine in 100 ml of H_2O. The temperature of the mixture was raised to 50° and the pH of the solution maintained at 9.5 by addition of 4M NaOH. When no further change of pH was observed the solution was diluted with H_2O to about 500 ml and introduced into a cation exchange column (*Dowex-50X8*; column length 30 cm; bed volume 400 ml; form H^+). The resin was washed with H_2O to neutrality and the product was eluted with 0.1M NaOH. The effluent solution was fractionated and the fractions were analyzed by acidimetric titration. The disubstituted product was contained in the nearly neutral fractions showing a buffer region around pH = 9. These fractions were evaporated under vacuum; 5 g (33% yield) of an oily product were obtained. All tentatives to crystallize the product failed and it was therefore used in its crude form for the synthesis of cobalt(III) complexes. ^{1}H-NMR (60 MHz; D_2O): 1.9 (*d*, *J* = 7.5, 6H); 3.1 (*s*, 6H); 3.9 (*s*, 4H); 4.7–5.2 (*m* unresolved, 2H); 7.3 (*d*, *J* = 7.5, 2H); 8.0–8.2 (*m* unresolved, 1H).

2.3. *2,6-Bis[(3S)-3-carboxy-4-methyl-2-azapentyl]pyridine.* 2,6-Bis(bromomethyl)pyridine (5.5 g, 0.02 mol) [9] were dissolved in 100 ml of EtOH and mixed with 100 ml of an aq. solution containing 4.9 g (0.04 mol) of (*S*)-valine. The pH of the mixture was fixed at 10 by addition of 2M NaOH. Further NaOH was added to maintain the pH at the initial value. When no more comsumption of NaOH occured, the mixture was neutralized with HCl and introduced into a cation exchange column. Washing and elution were performed as indicated in *1.2*. The fractions showing negative optical rotation in neutral solution were collected and evaporated under vacuum. The product solidified on the addition of Et_2O; yield 4.5 g (63%). The ligand was used without further purification for the synthesis of the corresponding aqua-cobalt(III) complex.

2.4. *Aqua[2,6-bis(3-carboxy-1,2-dimethyl-2-azapropyl)pyridine]cobalt(III) hexafluorophosphate.* To 300 ml of an aq. solution containing 11.2 g (0.036 mol) of 2,6-bis(3-carboxy-1,2-dimethyl-2-azapropyl)pyridine, prepared as indicated in *1.2*, 14 g (0.04 mol) of freshly prepared $Na_3[Co(CO)_3]\cdot 3\ H_2O$ and 2 g of active charcoal were added. The temperature of the mixture was maintained during 3 h at 50° and the pH of the solution was kept at 6.5 by addition of AcOH. The solution was filtered on *Celite* and the filtrate was poured into a cation exchange column *SPC-25 Sephadex* (Na^+). The column was washed with H_2O and the complex eluted with 1% NaCl. From the concentrated effluent solution, NaCl was eliminated by elution on *Sephadex G-10*. The salt-free solution was evaporated to dryness and the complex dissolved in the minimum amount of 10% NH_4PF_6. By slow evaporation of the solution, two types of crystals were formed. The complex containing the racemic ligand crystallized as fine red needles, whereas the complex containing the *meso*-ligand formes large dark red plates. The two crystalline forms were separated manually and both complexes were purified by recrystallization from 10% NH_4PF_6. The purity of the compounds were checked by ^{1}H-NMR measurements (*cf. Fig. 2* and *3*). Anal. calc. for rac-$[Co(C_{15}H_{21}N_3O_4)]PF6\cdot 2H_2O$ (565) (acidimetric titration: $pK_a = 8.3$; M = 569 g/mol): Co 10.40, C 31.87, H 4.81, N 7.43; found: Co 10.80, C 31.84, H 4.35, N 7.40.

2.5. *Chloro(2,6-bis(3-carboxy-1,2-dimethyl-2-azapropyl)pyridine)cobalt(III).* Racemic aqua(2,6-bis(3-carboxy-1,2-dimethyl-2-azapropyl)pyridine)cobalt(III) hexafluorophosphate (0.6 g) was dissolved in 50 ml of 37% HCl. The acid was slowly evaporated in an oil bath at 120° and the residue dissolved in EtOH. The solution of the chloro complex was again evaporated under vacuum to dryness. After dissolution in the minimum volume of hot EtOH, the complex crystallized on standing in the refrigerator. Violet crystals, yield 0.2 g (47%). Anal. calc. for $[Co(C_{15}H_{21}N_3O_4)Cl]$ (401): C 44.80, H 5.27, N 10.46; found: C 44.50, H 5.37, N 10.11.

2.6. *Aqua(2,6-bis[(3S)-3-carboxy-4-methyl-2-azapentyl]pyridine)cobalt(III) hexafluorophosphate.* The complex was prepared as indicated under *1.4* from 2,6-bis[(3*S*)-3-carboxy-4-methyl-2-azapentyl]pyridine. The product was characterized by ^{1}H-NMR, CD and visible spectra. ^{1}H-NMR (200 MHz; DMSO): 1.1 (*d*, *J* = 7.5, 6H); 1.2 (*d*, *J* = 7.5, 6H); 2.3 (*m* unresolved, 2H); 3.2 (*d*, *J* = 7.5, 2H); 4.4 and 5.1 (*AB*-system, *J* = 15, 2 2H); 6.2 (br. *s*, 2H); 7.5 (*s*, 2H); 7.7 (*d*, *J* = 7.5, 2H); 8.2 (*t*, *J* = 7.5, 1H). D_2O-addition leads to the disappearance of the signals at 7.5 and 6.2 ppm.

3. *Partial Resolution of the Racemic Aqua[2,6-bis(3-carboxy-1,2-dimethyl-2-azapropyl)pyridine]cobalt(III) Complex.* An aq. solution containing 1 g of the racemic complex was introduced into a *SP-C25 Sephadex* cation exchange column (Na^+, length 150 cm, diameter 3.5 cm). The fixed complex was eluted with 0.15M potassium (+)-antimonyltartrate. The eluted band was divided in two equal parts which were introduced separately into a cation exchange column (*Dowex-50*, Na^+). The column was washed with H_2O and the complex eluted with 2% NaCl. The concentrate effluent solution was freed from excess salt by passing through a *Sephadex G-10* column. The optical enrichment of the two fractions was controlled by the determination of the specific rotation. Values of $[\alpha]_{436} \approx 200°$ were obtained (calculated for the hexafluorophosphate, M = 565 g/mol).

Further enrichment could be achieved in the following way: the salt-free solution containing the enriched complex was evaporated to dryness under vacuum and the residue was dissolved in a small amount of 10% $NaClO_4$. In a first step almost racemic product crystallized, whereas the optically active compound remained in solution. When the specific rotation of the solution exceeded values of about $[\alpha]_{436} = 500°$ the optically active complex crystallized preferentially. This product was then recrystallized from 10% $NaClO_4$ solution as long as the optical activity of the crystallized solid and the mother solution were different. By this procedure, products showing specific rotations of $[\alpha]_{436} = +1050°$ and $-1010°$ ($c = 0.2$; H_2O; r.t.) were obtained.

REFERENCES

[1] *R. Deschenaux & K. Bernauer*, Helv. Chim. Acta *67*, 373 (1984).
[2] *M. Brorson, T. Damhus & C.E. Schäffer*, Inorg. Chem. *22*, 1569 (1983).
[3] *K. Bernauer, R. Deschenaux & T. Taura*, Helv. Chim. Acta *66*, 2049 (1983).
[4] *K. Bernauer*, Topics Curr. Chem. *65*, 1–35 (1976).
[5] *H. Stoeckli, L. Brehm, Ph. Pousaz, K. Bernauer & H.-B. Bürgi*, Helv. Chim. Acta, to be published.
[6] *L.N. Schoenberg, D.W. Cooke & C.F. Liu*, Inorg. Chem. *7*, 2386 (1977).
[7] *K. Bernauer & C. Soerensen*, Helv. Chim. Acta, to be published.
[8] *R. Lukes*, Collect. Czech. Chem. Commun. *24*, 36 (1959).
[9] *T. Baker*, J. Chem. Soc. *1958*, 3594.

HELVETICA CHIMICA ACTA

EDENDA CURAT SOCIETAS CHIMICA HELVETICA

Volumen 68
Fasciculus primus
1985

22. The Crystal Structure of Racemic and *meso*-Diastereoisomers of Aqua[2,6-bis(3-carboxy-1,2-dimethyl-2-azapropyl)pyridine]-Co(III)·Hexafluorophosphate·Di- and Monohydrate, Respectively

by **Helen Stoeckli-Evans***, **Lotte Brehm**[1]), **Philippe Pousaz**, and **Klaus Bernauer**

Institut de Chimie de l'Université de Neuchâtel, Avenue de Bellvaux 51, CH-2000 Neuchâtel

and **Hans-Beat Bürgi**

Laboratorium für Chemische und Mineralogische Kristallographie, Freiestrasse 3, CH-3012 Bern

(5.XI.84)

VERLAG HELVETICA CHIMICA ACTA
4002 BASEL, SCHWEIZ

SEPARATUM

22. The Crystal Structure of Racemic and *meso*-Diastereoisomers of Aqua[2,6-bis(3-carboxy-1,2-dimethyl-2-azapropyl)pyridine]-Co(III)·Hexafluorophosphate·Di- and Monohydrate, Respectively

by **Helen Stoeckli-Evans***, **Lotte Brehm**[1]), **Philippe Pousaz**, and **Klaus Bernauer**

Institut de Chimie de l'Université de Neuchâtel, Avenue de Bellvaux 51, CH-2000 Neuchâtel

and **Hans-Beat Bürgi**

Laboratorium für Chemische und Mineralogische Kristallographie, Freiestrasse 3, CH-3012 Bern

(5.XI.84)

Synthesis of the pentadentate ligand 2,6-bis(3-carboxy-1,2-dimethyl-2-azapropyl)pyridine yields a mixture of the racemic and *meso*-isomers which it was difficult to separate by column chromatography. When the cationic Co(III)-complex of this ligand was crystallized with hexafluorophosphate as anion, two distinct crystalline forms were produced. The complex of the racemic ligand, **1**, has C_2 symmetry and is a dihydrate; $a = 8.999(8)$, $b = 12.047(6)$, $c = 20.65(1)$ Å, orthorhombic, space group *Pccn*, $Z = 4$, $R = 0.074$ for 1439 observed reflections. The complex of the *meso*-ligand, **2**, shows two independent molecules (**2A** and **2B**) per asymmetric unit, both monohydrates with a resolved disordered H_2O molecule in **2A**; $a = 10.109(4)$, $b = 12.835(2)$, $c = 16.651(3)$ Å, $\alpha = 89.5(1)°$, $\beta = 84.7(3)°$, $\gamma = 88.6(3)°$, triclinic, space group $P\bar{1}$, $Z = 4$, $R = 0.054$ for 4198 observed reflections. The coordination around the Co-atom is distorted octahedral in both complexes, with the coordinated H_2O molecule *trans* to the pyridine N-atom. In the racemic form of the complex, **1**, the pyridine ring is twisted about the Co-N(1) bond with respect to the plane defined by atoms Co, N(1), O(W1), N(2) and N(2P) by 17.2(2)°. In the *meso*-form of the complex, **2**, the CH_3 substituent C(8P) on atom C(4P), is now axial with respect to the 5-membered chelate ring. As a result of steric hinderance between atom O(1) and CH_3(8P), the pyridine ring has been displaced from the best mean-plane formed by atoms Co, O(W1), N(2) and N(2P). The principal axis of the pyridine ring C(3)...N(1), makes an angle of 14.1(1)° (mean) with this plane. At the same time the pyridine ring is twisted about axis C(3)...N(1) with respect to this plane by 19.7(1)° (mean).

Introduction. – In [1], *Bernauer* and *Pousaz* have described the synthesis and the chemical and spectral analyses of racemic and *meso*-aqua[2,6-bis(3-carboxy-1,2-dimethyl-2-azapropyl)pyridine]Co(III)·hexafluorophosphate (henceforth **1** and **2**). They were prepared as suitable models for the study of stereoselective effects in an inner-sphere electron-transfer reaction between Co(III)- and Fe(II)-complexes, mediated by a bridging atom or group common to the coordination sphere of both molecules. To detect and to discuss such stereoselective effects, it is important to use model compounds which exhibit a unique and definite absolute configuration. It is also necessary to know the exact position of the groups which are especially important in determining the stereochemical interactions in the reactive binuclear intermediate. This stereoselectivity should constitute a precious tool for the study of reaction mechanisms, in particular with respect to the exact geometry of the transition state.

Experimental. – Compounds **1** and **2** were crystallized from a 10% aq. soln. of ammonium hexafluorophosphate. Preliminary *Weissenberg* and precession photographs indicated that crystals of **1** were orthorhombic, space group *Pccn*; crystals of **2** were triclinic, space group $P\bar{1}$ (by successful refinement). Accurate cell dimensions were obtained by least-squares from the setting of 14 (for **1**) and 25 (for **2**) reflections well-distributed in the *Ewald*

[1]) Permanent address: Royal Danish School of Pharmacy, Department of Chemistry BC, Universitetsparken 2, DK-2100 Copenhagen.

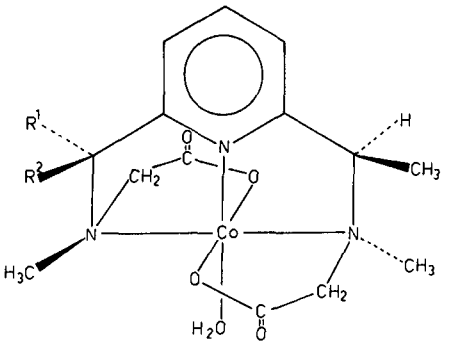

1 $R^1 = CH_3$, $R^2 = H$; (1*RS*, 1'*RS*) (racemic complex)
2 $R^1 = H$, $R^2 = CH_3$; (1*R*, 1'*S*) (*meso*-complex)

Table 1. *Summary of Crystal Data, Intensity Collection and Refinement Procedures*

Formula	**1** (Racemic complex) $C_{15}H_{23}N_3O_5Co^+ \cdot PF_6^- \cdot 2H_2O$	**2** (*meso*-Complex) $C_{15}H_{23}N_3O_5Co^+ \cdot PF_6^- \cdot H_2O$
Mol.wt.	565.3	547.3
Crystal form	red needles	red plates
Dimensions (mm)	0.4 × 0.2 × 0.2	0.08 × 0.3 × 0.3
Crystal system	orthorhombic	triclinic
Space group	*Pccn*	$P\bar{1}$
a (Å)	8.999(8)	10.109(4)
b (Å)	12.047(6)	12.835(2)
c (Å)	20.65(1)	16.651(3)
α (°)	90.0	89.5(1)
β (°)	90.0	84.7(3)
γ (°)	90.0	88.6(3)
V (Å^3)	2238.7	2150.5
Z	4	4
d_m (Mg m^{-3})	1.67	1.64
d_c (Mg m^{-3})	1.667	1.690
F_{000}	1160	1120
Radiation	MoK_α-graphite-monochromated, λ = 0.7107 Å	
μ (cm^{-1})	8.6	8.6
Scan method	ω-scan	ω-scan
θ_{max}	25°	24°
Data collected	h, k, l	$\pm h, \pm k, l$
No. independent reflections	2466	5273
No. observed reflections, $I > 2\sigma(I)$	1450	4204
No. reflections/No. parameters	9.0	5.4
Refinement	full-matrix least-squares	blocked-matrix least-squares (2 × 390)
No. of reflections in final cycle	1439	4198
Max. shift/e.s.d.	0.31	1.27
Av. shift/e.s.d.	< 0.1	< 0.4
R	0.074	0.054
R_w	0.078	0.056
$w = (\sigma^2(F_o) + g(F_o)^2)^{-1}$,	$g = 2.5 \times 10^{-4}$	2.6×10^{-4}
Function minimized	$\Sigma w(\|F_o\| - k\|F_c\|)^2$	idem
Heights in Final	+ 1.8	+ 0.6
Difference Map (eÅ^{-3})	− 0.8	− 0.5

sphere, measured on *Enraf-Nonius CAD4* diffratometers. The crystal data and details of the data-collection and structure-refinement procedures are given in *Table 1*. The structures were solved by means of *Patterson* and difference *Fourier* syntheses. SHELX-76 [2] was used for all calculations. In both complexes the PF_6^- anions were disordered. This disorder was resolved in **1** and the model chosen for it was one in which the atoms occupied the most populated sites. No further refinement of this description was attempted. In **1**, H-atoms were included in idealized positions and treated as 'riding atoms' for CH and CH_2 protons, and as 'rigid groups' for CH_3 protons (C–H = 1.08 Å) [U_{iso} (refined values) = 0.091 and 0.097 Å^2, respectively]. The H-atoms of the coordinated H_2O molecule O(W1) were located in a difference map, only U_{iso} was refined (final value 0.057 Å^2). H-atoms of the H_2O molecule of crystallization, O(W2), were located in a difference map but not refined [U_{iso} (fixed) = 0.09 Å^2]. In **2** all the H-atoms, except those of the H_2O molecule of crystallization, were located in difference maps and refined isotropically. In **2**, the H_2O molecules of crystallization were disordered; in **2A** this disorder was clearly resolved (occupancy 0.75:0.25). A small number of reflections (11 for **1**, 6 for **2**), probably suffering from extinction, were removed in the final cycle of refinement. Complex neutral-atom scattering factors were taken from [3].

Discussion. – Final positional and equivalent isotropic thermal parameters are given in *Tables 2a* and *2b*. Selected bond distances and angles are given in *Table 3*. Torsion angles of the 5-membered chelate rings are given in *Table 4*. Perspective views of cations **1** and **2A**, illlustrating the number schemes used, are given in *Figs. 1* and *2*, respectively (prepared using ORTEP [4]). In all three cations (**1**, **2A** and **2B**), the coordinated H_2O molecule, O(W1), is *trans* to the pyridine N-atom. The racemic complex **1** has crystallographic C_2 symmetry with atoms Co, N(1), C(3) and O(W1) lying on the 2-fold axis. The coordination around the Co-atom is distorted octahedral in all three cations. The distortions are greater in the *meso*-complex **2**, as a result of steric hinderance between atom O(1) and the CH_3 substituent at atom C(4P), which in **2** is axial with respect to the 5-membered chelate ring. Angles N(2)– and N(2P)–Co–N(1) have a mean value of

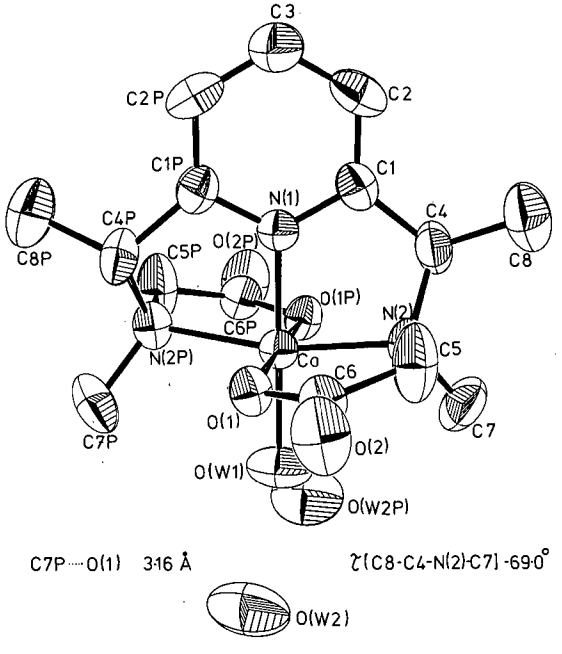

Fig. 1. *A perspective view of aqua[2,6-bis((1RS,1'RS)-3-carboxy-1,2-dimethyl-2-azapropyl)pyridine]cobalt(III)* (**1**) *showing the numbering scheme and vibrational ellipsoids* (50% probability). Atoms C1 and C1P *etc.* are related by a crystallographic 2-fold axis.

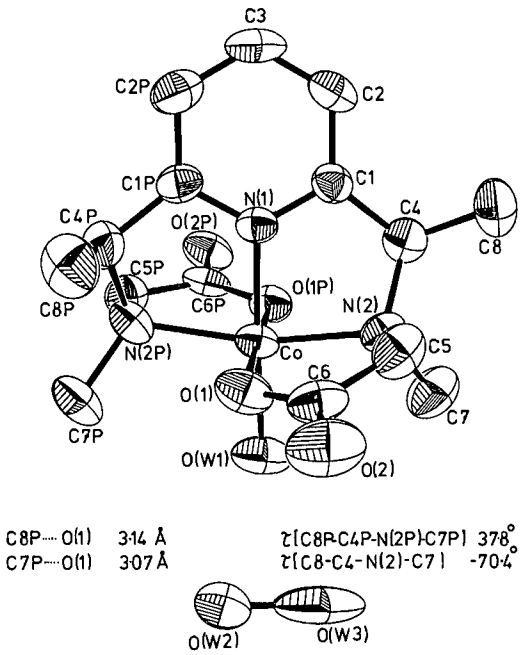

Fig. 2. *A perspective view of aqua [2,6-bis((1R,1'S)-3-carboxy-1,2-dimethyl-2-azapropyl)pyridine]cobalt(III)* (**2A**) *showing the numbering scheme and vibrational ellipsoids* (50% probability). In **2** atoms C1 and C1P *etc.* are crystallographically independent.

82.9(1)° in the three cations. This is slightly less than in Azido[2,6-bis(aminomethyl)pyridine](1,3-diaminopropane-2-ol)Co(III)·2 Br [5] where the mean of the same angles was 84.5°. In cation **1**, the planes containing atoms Co, N(1), N(2), N(2P), O(W1) and Co, N(1), O(1), O(1P), O(W1) are perfectly planar for reasons of site symmetry. The pyridine ring is twisted about the Co–N(1) bond with respect to the former plane by 17.2(2)°. In cation **1**, angles O(1)– and O(1P)–Co–N(1) are 91.7(2)°. In cations **2A** and **2B**, these angles are (mean) 97.5(1)° and 86.9(1)°, respectively. To reduce the steric hinderance mentioned above the pyridine ring has been displaced from the vertical plane containing atoms Co, O(W1), N(2) and N(2P). The principal axis of the pyridine ring, N(1)...C(3), is inclined to this plane by 14.0° in **2A** and 14.2° in **2B**. Atom N(1) is displaced from the plane by 0.16 Å in **2A** and 0.19 Å in **2B**. The pyridine ring is twisted about axis N(1)...C(3) such that the dihedral angle between the vertical plane and the pyridine ring is 19.8(2)° in **2A** and 19.6(2)° in **2B**. The horizontal planes containing atoms Co, N(2), N(2P), O(1) and O(1P) are non-planar in all three cations and exhibit tetrahedral deformations about the Co-atoms.

The effects of steric hinderance can also be seen in the torsion angles of the 5-membered chelate rings in the three cations *(Table 4)*. In **1**, chelate ring Co, N(1), C(1), C(4), N(2) is intermediate between a C_s [N(2)] envelope and a C_2 [N(1)] half-chair conformation. In **2A** and **2B**, the same ring has a C_s [N(2)] envelope conformation. In **2**, chelate ring Co, N(1P), C(1P), C(4P), N(2P) is much flatter than the same ring in **1** and now has a C_2 [N(1P)] half-chair conformation. In **1**, chelate ring Co, N(2), C(5), C(6), O(1) is flatter than the same ring in **2**, but all three rings have approximate C_s [C(5)] envelope conforma-

Table 2. *Final Positional* (× 10^4) *and Equivalent Isotropic Thermal* (× 10^3) *Parameters with Estimated Standard Deviations in Parentheses.* a) *Racemic complex* **1**, b) meso-*complex* **2**. $U_{eq} = 1/3 \sum_i \sum_j U_{ij} a_i^* a_j^* \mathbf{a}_i \mathbf{a}_j$.

a)

	x/a	*y/b*	*z/c*	U_{eq}(Å^2)		*x/a*	*y/b*	*z/c*	U_{eq}(Å^2)
Co	7500	2500	3858(1)	35(1)	O(1)	6182(5)	1306(4)	3884(2)	42(2)
O(W1)	7500	2500	4783(4)	65(3)	O(2)	3767(6)	903(5)	3866(4)	76(2)
N(1)	7500	2500	2968(3)	37(2)	C(7)	5512(11)	4292(8)	4281(4)	71(3)
C(1)	6745(8)	3302(6)	2660(4)	47(2)	C(8)	4778(10)	4785(9)	2858(5)	80(4)
C(2)	6728(9)	3319(8)	1993(4)	63(3)	O(W2)	5894(10)	1075(6)	5438(3)	105(3)
C(3)	7500	2500	1671(6)	78(5)	P	2500	2500	6274(6)	179(3)
C(4)	6071(9)	4134(7)	3129(4)	56(3)	F(1)	3970(13)	2963(7)	6018(8)	186(6)
N(2)	5752(6)	3506(5)	3744(3)	41(2)	F(2)	1781(9)	3627(6)	6370(5)	161(4)
C(5)	4458(9)	2754(6)	3664(6)	74(4)	F(3)	3453(21)	2870(12)	6957(11)	297(11)
C(6)	4795(8)	1563(6)	3829(4)	47(2)					

b)

	2A				**2B**			
	x/a	*y/b*	*z/c*	U_{eq}(Å^2)	*x/a*	*y/b*	*z/c*	U_{eq}(Å^2)
Co	−2940(1)	2968(1)	−5575(1)	40(1)	1685(1)	1896(1)	9163(0)	41(1)
O(W1)	−4562(5)	2576(4)	−4964(3)	62(1)	−210(5)	2055(5)	9343(3)	61(3)
N(1)	−1374(5)	3437(3)	−6093(3)	37(1)	3499(5)	1604(3)	8990(3)	42(1)
C(1)	−347(6)	3519(5)	−5653(4)	41(1)	4232(6)	1659(4)	9620(4)	46(1)
C(1P)	−1394(6)	3851(5)	−6833(4)	43(1)	3966(7)	1194(5)	8277(4)	56(2)
C(2)	782(7)	4007(6)	−5992(5)	56(2)	5539(8)	1320(6)	9523(6)	72(2)
C(2P)	−298(8)	4350(6)	−7180(5)	60(2)	5276(9)	818(7)	8183(8)	83(3)
C(3)	797(8)	4410(6)	−6756(5)	64(2)	6016(10)	889(7)	8801(7)	89(3)
C(4)	−608(7)	3146(5)	−4815(4)	48(2)	3441(7)	2023(5)	10369(4)	51(2)
C(4P)	−2660(7)	3678(6)	−7199(4)	54(2)	2979(8)	1213(6)	7662(4)	64(2)
N(2)	−1738(5)	2398(4)	−4795(3)	46(1)	2264(5)	2630(4)	10121(3)	44(1)
N(2P)	−3745(5)	3638(4)	−6510(3)	49(1)	1633(6)	1147(4)	8121(3)	57(1)
C(5)	−1275(9)	1349(6)	−5117(5)	61(2)	2644(9)	3678(5)	9820(5)	56(2)
C(5P)	−4091(8)	4741(5)	−6244(5)	50(2)	1342(13)	51(7)	8359(5)	80(2)
C(6)	−2175(7)	958(5)	−5710(5)	58(2)	1980(7)	3974(5)	9083(4)	55(2)
C(6P)	−3565(6)	4999(5)	−5471(4)	44(1)	1495(6)	−194(5)	9219(4)	50(2)
O(1)	−2878(4)	1640(3)	−6039(3)	56(1)	1675(5)	3217(3)	8651(3)	58(1)
O(1P)	−3103(4)	4264(3)	−5059(3)	46(1)	1540(4)	592(3)	9694(2)	48(1)
O(2)	−2152(6)	28(4)	−5874(4)	86(2)	1805(5)	4898(4)	8892(3)	75(1)
O(2P)	−3603(4)	5919(3)	−5250(3)	58(1)	1533(5)	−1093(3)	9436(3)	66(1)
C(7)	−2392(11)	2296(8)	−3963(5)	70(2)	1211(8)	2715(8)	10801(5)	61(2)
C(7P)	−4960(8)	3120(7)	−6730(7)	67(2)	554(10)	1565(8)	7624(5)	76(2)
C(8)	603(12)	2773(11)	−4417(8)	78(3)	4273(11)	2577(9)	10936(6)	78(2)
C(8P)	−2515(10)	2712(8)	−7736(6)	76(2)	3180(13)	2156(9)	7116(6)	82(3)
O(W2)[a]	−5968(11)	939(8)	−5202(7)	83(3)	−1397(10)	3834(6)	9780(6)	180(3)
O(W3)[a]	−5361(22)	767(20)	−442(19)	113(7)				
P	−8164(2)	1096(2)	−7010(1)	61(1)	−3832(2)	4193(2)	8204(1)	77(1)
F(1)	−8172(6)	1555(5)	−6144(3)	119(2)	−3608(5)	4390(5)	7276(3)	107(1)
F(2)	−9596(6)	1464(7)	−7053(4)	158(2)	−2774(7)	5015(5)	8350(3)	142(2)
F(3)	−8162(6)	679(5)	−7888(3)	122(2)	−4051(6)	4025(7)	9134(3)	165(2)
F(4)	−6704(6)	814(8)	−6970(6)	213(3)	−4872(9)	3400(6)	8109(5)	191(3)
F(5)	−7736(10)	2181(7)	−7329(4)	194(3)	−4966(8)	5056(7)	8256(5)	175(3)
F(6)	−8543(13)	74(6)	−6708(5)	231(4)	−2704(8)	3425(7)	8144(5)	184(3)

[a]) Occupancy: O(W2) 0.75; O(W3) 0.25, for **2A** only.

Table 3. *Selected Bond Distances* (Å) *and Angles* (°) *in* **1**, **2A** *and* **2B**

	1	2A	2B
Co–N(1)	1.838(7)	1.843(5)	1.859(5)
Co–N(2)	2.000(5)	1.983(5)	2.000(5)
Co–N(2P)		2.000(5)	1.997(5)
Co–O(1)	1.865(4)	1.875(5)	1.891(5)
Co–O(1P)		1.876(5)	1.890(4)
Co–O(W1)	1.909(8)	1.923(5)	1.918(5)

	1	2A	2B
N(1)–Co–N(2)	83.2(2)	82.8(2)	81.6(2)
N(1)–Co–N(2P)		83.5(2)	83.3(2)
N(1)–Co–O(1)	91.7(2)	97.2(2)	97.8(2)
N(1)–Co–O(1P)		86.8(2)	87.0(2)
N(1)–Co–O(W1)	180.0	174.8(2)	174.4(2)
N(2)–Co–O(1)	88.3(2)	87.3(2)	86.6(2)
N(2P)–Co–O(1P)		88.0(2)	88.1(2)
N(2)–Co–O(1P)	91.7(2)	92.4(2)	94.1(2)
N(2P)–Co–O(1)		93.3(2)	92.5(2)
N(2)–Co–O(W1)	96.8(2)	95.8(2)	101.3(2)
N(2P)–Co–O(W1)		98.0(2)	94.1(2)
O(1)–Co–O(W1)	88.3(2)	87.7(2)	87.1(2)
O(1P)–Co–O(W1)		88.3(2)	88.1(2)
N(2)–Co–N(2P)	166.4(2)	166.2(2)	164.5(2)
O(1)–Co–O(1P)	176.6(2)	175.9(2)	175.2(2)

Table 4. *Torsion Angles* (°) *for the 5-Membered Chelate Rings* (e.s.d. *ca.* 0.8°), *in* **1**, **2A** *and* **2B**

	1	2A	2B		2A	2B
Co–N(1)–C(1)–C(4)	3.3	– 3.9	– 3.6	Co–N(1P)–C(1P)–C(4P)	11.5	10.7
N(1)–C(1)–C(4)–N(2)	– 30.0	– 22.6	– 23.7	N(1P)–C(1P)–C(4P)–N(2P)	– 30.7	– 29.5
C(1)–C(4)–N(2)–Co	40.1	36.0	37.6	C(1P)–C(4P)–N(2P)–Co	34.5	33.7
C(4)–N(2)–Co–N(1)	– 32.1	– 31.2	– 32.2	C(4P)–N(2P)–Co–N(1P)	– 24.1	– 23.9
N(2)–Co–N(1)–C(1)	17.3	21.1	21.2	N(2P)–Co–N(1P)–C(1P)	7.9	8.0
Co–N(2)–C(5)–C(6)	12.0	18.8	23.3	Co–N(2P)–C(5P)–C(6P)	– 8.4	– 13.3
N(2)–C(5)–C(6)–O(1)	– 13.8	– 21.5	– 27.3	N(2P)–C(5P)–C(6P)–O(1P)	11.6	16.0
C(5)–C(6)–O(1)–Co	7.8	12.3	16.1	C(5P)–C(6P)–O(1P)–Co	– 8.3	– 9.6
C(6)–O(1)–Co–N(2)	– 0.4	– 0.4	– 1.4	C(6P)–O(1P)–Co–N(2P)	2.4	1.1
O(1)–Co–N(2)–C(5)	– 6.7	– 10.8	– 12.8	O(1P)–Co–N(2P)–C(5P)	3.7	7.0

tions. Atom O(2) is displaced below the best mean-plane by 0.14, 0.28 and 0.37 Å in **1**, **2A** and **2B**, respectively. Chelate ring Co, N(2P), C(5P), C(6P), O(1P) also has an approximate C_s [C(5)] envelope conformation in **2B** but a C_2 [Co] half-chair conformation in **2A**. However, atom O(2P) is now displaced above the chelate ring mean-plane by 0.20 and 0.21 Å in **2A** and **2B**, respectively.

The mean Co–N(pyridine) distance in the three cations is 1.847(3) Å. This is close to the distance observed in the above mentioned complex, 1.845 Å [5] and in carbonatohydroxo(2,2′:6′,2″-terpyridyl)Co(III) · tetrahydrate [6], 1.846(8) Å. In the three cations, the mean Co–O(Water) distance [1.917(3) Å], the mean of the N(2)– and N(2P)–Co distances [1.997(2) Å] and the mean Co–O(carboxylate) distance [1.879(3) Å] are similar to those observed in aquo(ethylenediaminetriacetatoacetic acid)Co(III) · trihydrate [7]. In **2**,

steric hinderance has also resulted in a closing of angle C(1P)–C(4P)–C(8P) compared to angle C(1)–C(4)–C(8). For the three cations, the mean value of the latter angle is 114.(4)°, whereas the mean value of the former angle for **2A** and **2B** is 110.1(5)°. In **1**, torsion angle C(8)–C(4)–N(2)–C(7) is −69.0(8)° compared to a mean value of −71.3(6)° in **2A** and **2B**. Torsion angle C(8P)–C(4P)–N(2P)–C(7P) has a mean value of 36.7(6)° in **2A** and **2B**. The majority of the remaining bond distances and angles in the three cations are similar to those observed in related structures [6–8].

In **1**, two H_2O molecules of crystallization, related by the 2-fold axis, are H-bonded to the coordinated H_2O molecule, O(W1). Angles N(2)– and N(2P)–Co–O(W1) are 98.6(2)°. In **2**, there is only on H_2O molecule of crystallization per independent molecule. They too are H-bonded to O(W1) but occupy different locations with respect to bond Co–O(W1). Angles N(2)– and N(2P)–Co–O(W1) now differ, with the larger angle facing the H_2O molecule of crystallization. This is illustrated in *Fig. 2* where angle N(2P)–Co–O(W1) is the larger by 2.2°. In **2B**, the situation is reversed with angle N(2)–Co–O(W1) the larger by 7.2°, see *Table 3*. In the crystals of both complexes, the molecules are linked into chains, extending in the *b* direction, by intermolecular H-bonds. Details are given in *Table 5*. There are no other short intermolecular contacts between non-H-atoms in the crystals of either complex.

Table 5. *H-Bonding, Distances* (Å) *and Angles* (°)

A–H ... B	A–H	A ... B	H ... B	< AHB
Racemic complex **1**				
O(W1)–H(W1) ... O(W2)	0.78(1)	2.62(1)	1.85(1)	170(2)
O(W2)–H2(W2) ... O(2)[a])	0.72(1)	2.80(1)	2.25(1)	134(2)
meso-Complex **2A**				
O(W1)–H2(W1) ... O(W2)	0.91(8)	2.62(1)	1.71(8)	176(2)
O(W1)–H1(W1) ... O(2P)[b])	0.83(7)	2.65(1)	1.82(7)	174(2)
O(W2)–* ... O(2)[a])		2.80(1)		
meso-Complex **2B**				
O(W1)–H1(W1) ... O(W2)	0.80(9)	2.63(1)	1.85(9)	164(2)
O(W1)–H2(W1) ... O(2P)[c])	0.84(7)	2.64(1)	1.81(7)	169(6)
O(W2)–* ... O(2)[d])		2.75(1)		

Symmetry operations: [a]) 1 − x, − y, 1 − z; [b]) 1 − x, − 1 − y, 1 − z; [c]) − x, − y, 2 − z; [d]) − x, 1 − y, 2 − z.
* H-atoms not located.

Tables of final observed and calculated structure factors *etc.* are available from *H. St-E.* We wish to thank Mr. *F. Hansen* (Copenhagen) for technical assistance and the *Danish National Science Research Council* (grant No. 11/1837).

REFERENCES

[1] K. Bernauer, P. Pousaz, *Helv. Chim. Acta* **1984**, *67*, 796.
[2] G.M. Sheldrick, SHELX-76, A Programme for Crystal Structure Determination. Univ. of Cambridge, England, 1976.
[3] International Tables for X-ray Crystallography, Kynoch Press, Birmingham, **1974**, Vol. IV.
[4] C.K. Johnson, ORTEP II, Report ORNL-5138, Oak Ridge National Laboratory, Tennessee, 1976.
[5] U. Tinner, Thesis Dr. es Sc., ETH Zürich, No. 6463, 1979.
[6] E.S. Kucharski, B.W. Skelton, A.H. White, *Aust. J. Chem.* **1978**, *31*, 47.
[7] H. Okazaki, K. Tomoika, H. Yoneda, *Inorg. Chim. Acta* **1983**, *74*, 169.
[8] L. Randaccio, N. Bresciani-Pahor, P.J. Toscano, L.G. Marzilli, *Inorg. Chem.* **1981**, *20*, 2722; *J. Am. Chem. Soc.* **1981**, *103*, 6347.

146. Stereoselectivity in Reactions of Metal Complexes

Part X[1])

Kinetics and Stereoselectivity of the Inner-sphere Electron-Transfer Reaction between $[Co(bamap)H_2O]^+$ (bamap = 2,6-Bis(3-carboxy-1,2-dimethyl-2-azapropyl)pyridine) and Optically Active Iron(II) Complexes

by **Klaus Bernauer***, **Philippe Pousaz**[2]), **Joelle Porret**, and **André Jeanguenat**

Laboratoire de Chimie Inorganique et Analytique de l'Université de Neuchâtel, Bellevaux 51, CH-2000 Neuchâtel

(20. IV. 88)

The kinetics of the electron-transfer reaction between racemic or optically active $[Co(bamap)H_2O]^+$ and optically active Fe^{2+} complexes of the three new pentadentate ligands bamap, alamp, and valmp has been investigated. All the reacting species show C_2 symmetry. With respect to aquo-Fe^{2+}, the reaction rate for the Fe^{2+} complexes is enhanced by a factor of 10^4 to 10^5, and the observed $k_{\Delta\Delta}/k_{\Lambda\Lambda}$ ratio is 1.0, 1.9, and 1.2, respectively. In all cases where stereoselectivity is observed, the reaction is faster between the complexes of opposite absolute configurations ($\Delta\Lambda$ or $\Lambda\Delta$) than between species with the same configuration ($\Lambda\Lambda$ or $\Delta\Delta$). The stereoselectivity effects are discussed on the basis of the structure of the transition state and the interatomic distances between the two metal centers at the moment of electron transfer.

1. Introduction. – It has been argued, that the stereoselectivity – even when the observed effects are small – may be an important argument in the discussion of mechanistic features in electron-transfer reactions [2–4]. However, only a few other examples have been described [6–14] since the publication of the first example of an electron-transfer reaction, for which stereoselectivity was unambiguously demonstrated [5]. All these examples deal with reactions following an outer-sphere mechanism.

In the present paper, we relate the measurements of electron transfer between a Co(III) and an Fe(II) center, which are known to proceed generally by an inner-sphere mechanism *via* a bridged intermediate [15]. In outer-sphere reactions, stereoselectivity effects can appear in the formation of the precursor complex as well as in the electron transfer itself [7]; this may also be the case for an inner-sphere reaction with respect to the formation of the bridged intermediate or to the electron transfer which follows the pre-equilibrium.

The interpretation of the observed stereoselectivity effects is often difficult for the following reasons: *i)* the effects are, in general, small and represent only a minor fraction of the binding energies of the reactive intermediates, *ii)* several diastereoisomeric struc-

[1]) Part IX: [1].

[2]) Part of the Ph. D. thesis of *Ph. P.*, Université de Neuchâtel.

tures of almost the same stability may be considered for the intermediate so that the real structure of the latter is not known and *iii)* the effects in the pre-equilibrium and in the electron transfer may direct in opposite directions.

To eliminate these factors or at least to diminish their influence, the ligands, constituting the coordination sphere of the reacting compounds, should satisfy several conditions, the most important of which are the following: *i)* the ligand used should occupy all the coordination sites of both metal centers except those occupied by the bridging group, *ii)* the complex formed by the ligand should exist as only one goemetrical isomer, *iii)* complex formation with the optically active derivatives of the ligands must be completely diastereoselective, with inert as well as with labile systems, and *iv)* the absolute configuration of both reacting complexes must be known.

In [1], we have shown that linear pentadentate ligands derived from 2,6-bis(3-carboxy-2-azapropyl)pyridine as the basic framework should fulfill the conditions mentioned above, so that only one isomer of the inert Co(III) complexes is obtained, and that the optically active ligand forms complexes with a given absolute configuration. We may, therefore, assume that this will be true for labile complexes too. The ligands used in this work are shown below.

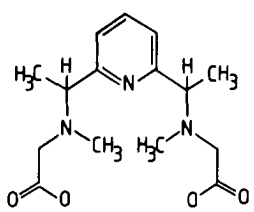

bamap

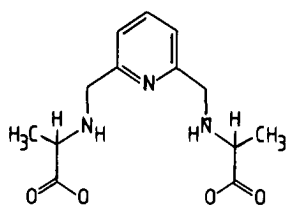

alamp

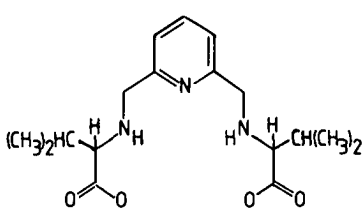

valmp

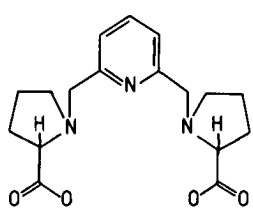

promp

2. Results. – 2.1. *Absolute Configuration.* A tentative proposal for the absolute configuration of the isomers of the $[Co(bamap)H_2O]^+$ and $[Co(valmp)H_2O]^+$ ions has been given on the basis of their CD and ^{1}H-NMR spectra [1]. To ensure this attribution of configuration, the new compound $[Co((S,S)\text{-promp})(py)]ClO_4$ was synthesized. By means of the cyclic structure of the pyrrolidine moieties, this ligand can coordinate as a pentadentate only, if the substituent on the α-C-atom in the aminocarboxylate chelate ring is in the *exo*-position. Together with the C_2-symmetric arrangement, the absolute configuration of the complex is unambiguously determined on the basis of the chirality of the amino-acid moiety *(Fig. 1)*.

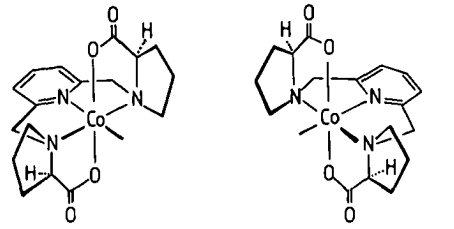

Δ-[Co(*R*, *R*)-promp]$^+$ Λ-[Co(*S*, *S*)-promp]$^+$

Fig. 1. *Absolute configuration of the [Co((R,R)-promp)]$^+$ and [Co((S,S)-promp)]$^+$ complexes*

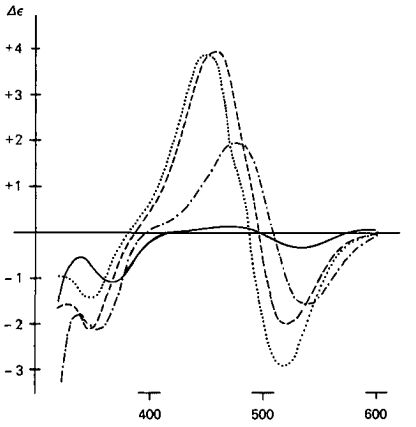

Fig. 2. *CD spectra of (−)$_{436}$-[Co(bamap)(H$_2$O)]ClO$_4$ (——); [Co((S,S)-alamp)(py)]ClO$_4$ (· · · · ·); [Co((S,S)-valmp)(py)]PF$_6$ (– – – –), and [Co((S,S)-promp)(py)]ClO$_4$ (– · – · – · –)*

The comparison of the CD spectra *(Fig. 2)* shows that the complexes derived from (*S*)-amino acids exhibit *Λ*-configuration, and that this is also the configuration of $(-)_{436}$-[Co(bamap)H_2O]$^+$. The structure of the latter is known from the X-ray diffraction analysis [16], indicating that (*S*)-chirality of the asymmetric C-atoms leads to the *Λ*-configuration for the complex. Furthermore, the pentacoordination of the ligand in [Co((*S*,*S*)-promp)(py)]$^+$ is confirmed by the NMR spectra, which is typical for an arrangement with C_2 symmetry.

2.2. *Kinetics of Electron Transfer.* When [Co(bamap)H_2O]$^+$ reacts with Fe^{2+} under pseudo-first-order conditions (presence of ascorbic acid) and in slightly acidic solution, strong auto-catalysis of the reaction is observed *(Fig. 3a)*. It can be attributed to the complexation of Fe^{2+} by the ligand which is set free during the reduction of the Co(III) complex. This ligand can bind to the different metal ions present in the solution (Fe^{2+}, Co^{2+}), depending upon their stability constants *(cf. Table 1)*. If a redox-inactive metal ion is present in excess, *e.g.* Zn^{2+}, the free ligand is trapped, and auto-catalysis disappears *(Fig. 3a)*. The reaction rate, then, corresponds to the reduction by the aquo-Fe^{2+}, allowing the determination of the corresponding rate constant.

When these rate constants are measured as a function of pH *(Fig. 3b)*, a proportional increase of the reaction rate is observed in slightly acidic solution, whereas, in more acidic solutions, the rate seems to reach a limiting value. This behaviour is in agreement with the rate law *(Eqn. 1)*:

$$k_{obs} = [Fe^{2+}]\{k_1 + K_H(k_2 - k_1)/(K_H + [H^+])\} \quad (1)$$

K_H being the acid dissociation constant of either the Co(III) complex or the aqua-Fe^{2+} ion, and k_1 and k_2 the rate constants for the reaction with the pH-independent and the pH-dependent reacting species, respectively. In the presence of ascorbic acid and for the pH range studied, $[Fe^{2+}] = c_{Fe^{2+}}$, $K_H \ll [H^+]$ and $k_1 \ll k_2$, *Eqn. 1*, then, becomes:

$$k_{obs} = (k_1 + k_2 K_H/[H^+])c_{Fe^{2+}} \quad (2)$$

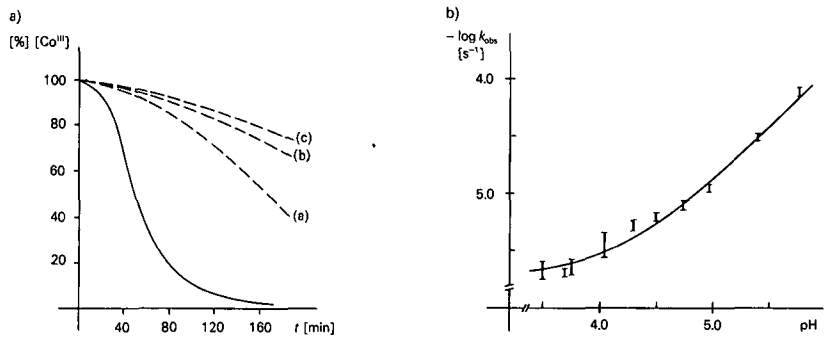

Fig. 3. a) *Electron transfer between [Co(bamap)(H$_2$O)]$^+$ and Fe^{2+} without* (——) *and in the presence of Zn^{2+}* (– – – –). Reaction conditions: [Co(bamap)(H$_2$O)]$^+$: $2.5 \cdot 10^{-3}$ M; Fe^{2+}: $2.6 \cdot 10^{-3}$ M; ascorbic acid: 0.02M; Zn^{2+}: 0.01M (a); 0.02M (b); 0.03M (c); pH = 4.0 (acetate buffer 0.1M); $T = 25°$. b) *Observed rate constants of the reaction between [Co(bamap)H$_2$O]$^+$ and Fe^{2+} in the presence of Zn^{2+} as a function of pH.* Reaction conditions: [Co(bamap)H$_2$O]$^+$: $2.5 \cdot 10^{-3}$M; Fe^{2+}: $2 \cdot 10^{-3}$M; Zn^{2+}: 0.1M; ascorbic acid: 0.02M; acetate buffer 0.1M; $T = 25°$.

The curve in *Fig. 3b* represents the calculated values obtained by using $k_1 = 9.0 \cdot 10^{-4}$ M$^{-1} \cdot$ s^{-1}, $k_2 = 12.0$ M$^{-1} \cdot$ s^{-1}, and $K_H = 5.0 \cdot 10^{-9}$ [1].

When free H$_2$bamap is added to the solution, a strong increase in the rate of electron transfer due to the formation of [Fe(bamap)] is observed. The concentration of the latter can be varied in two different ways: by changing the total concentration of Fe(II) and ligand, or by changing the pH of the solution. As is seen from the results given in *Fig. 4*, the values for the observed rate constants in both cases fall within the same straight line with a slope close to unity, indicating that the reaction rate depends on the pH value only, since a pH change modifies the concentration of [Fe(bamap)]. The values indicated in *Fig. 4* represent a variation of this concentration from 0.5 to 93% with respect to the total Fe^{2+}-bamap concentration. It seems, therefore, that in contrast to the case of aqua-Fe^{2+}, the electron transfer between the two complexed species takes place through the [Co(bamap)H$_2$O]$^+$; the reaction with the corresponding OH complex is not observed under the

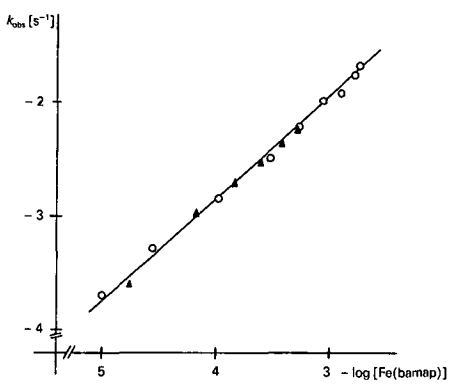

Fig. 4. *Observed rate constants of electron transfer between [Co(bamap)(H$_2$O)]$^+$ and [Fe(bamap)].* Reaction conditions: [Co(bamap)H$_2$O]$^+$: $2.5 \cdot 10^{-3}$ M; ascorbic acid: 0.02M; acetate buffer 0.1M; –▲–▲–: $c_{Fe^{2+}} = 0.72 \cdot c_{bamap}$, varied from $1 \cdot 10^{-3}$ M to $6 \cdot 10^{-3}$M. –○–○–: $c_{Fe^{2+}} = C_{bamap} = 2 \cdot 10^{-3}$ M, pH varied from 3.5 to 5.8.

Table 1. *Equilibrium Constants of the Systems M^{2+}–L^{2-} (M = Fe and Co) and Second-Order Rate Constants of Electron Transfer between $[Co(bamap)(H_2O)]^+$ and Optically Active FeL Complexes*

L^{2-}	pK_a [a]	pK_a [a]	$\log K_{ML}$ [a]		k^{TE} [b] $[M^{-1} \cdot s^{-1}]$	$k^{TE}(FeL)/k^{TE}(Fe^{2+})$ [c]
			Fe^{2+}	Co^{2+}		
bamap	8.91	9.61	11.93	13.72	13	$1.5 \cdot 10^4$
alamp	8.23	9.02	9.62	11.70	61	$6.8 \cdot 10^4$
valmp	8.02	9.28	10.44	11.80	10	$1.1 \cdot 10^4$

[a]) $T = 25°$; $\mu = 0.1$.
[b]) Reaction conditions as indicated in *Fig. 3a*.
[c]) For exact signification of $k^{TE}(Fe^{2+})$, see text.

prevailing reaction conditions (pH < 6). Fe(bamap) concentrations are calculated using the equilibrium constants reported in *Table 1*. These equilibrium constants, as well as the corresponding values of the optically active ligands (*S,S*)-alamp^{2-} and (*S,S*)-valmp^{2-}, were obtained by acidimetric titrations.

From the known concentrations of the three Fe(II) complexes, the pH-independent second-order rate constants of the overall electron-transfer reactions can be obtained.

2.3. *Stereoselectivity.* To demonstrate diastereoselectivity in the reaction between a kinetically inert Co(III) and a labile Fe(II) complex, there are two *Methods: a)* one enantiomer of the optically active Fe(II) complex is reacted with the racemic Co(III) complex; the stereoselectivity is, then, determined by the appearance of an excess of one of the two Co(III) enantiomers during the reaction; *b)* one enantiomer of one of the reacting complexes is measured individually with both enantiomers of the other complex.

The advantage of *Method a* consists in the fact that both enantiomers of the inert Co(III) complex react under completely identical conditions. Any – even very small – enantiomeric excess arising during the reaction gives, therefore, unequivocal evidence for the stereoselectivity of the reaction. *Method b* is useful, when the determination of enantiomeric excess is complicated by the presence of other optically active species. Its application is limited by the precision of the determination of reaction rates, and it is

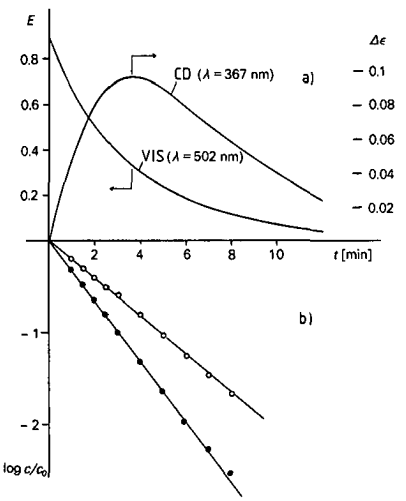

Fig. 5. *Stereoselectivity in the electron transfer reaction between (±)-$[Co(bamap)(H_2O)]^+$ and [Fe((S,S)-alamp)]. a)* Change of VIS and CD intensity. *b)* First-order rate plots of each enantiomer; concentration change calculated from VIS and CD variation. Reaction conditions: (±)-$[Co(bamap)(H_2O)]^+$: $2.5 \cdot 10^{-3}$ M; Fe^{2+}: $2.5 \cdot 10^{-3}$ M; (*S,S*)-alamp: 10^{-2} M; ascorbic acid: 0.1 M; pH = 4.0 (acetate buffer 0.1 M); $T = 25°$. –○–○–○–: (–)-$[Co(bamap)(H_2O)]^+$ ($k_{obs} = 3.2 \cdot 10^{-3}$ s^{-1}). –●–●–●–: (+)-$[Co(bamap)(H_2O)]^+$ ($k_{obs} = 5.5 \cdot 10^{-3}$ s^{-1}).

necessary that optical enantiomers of both complexes be available. In the present work, we applied both methods.

As an example for *Method a, Fig. 5a* shows the change of CD ($\lambda = 367$ nm) and VIS-absorption ($\lambda = 502$ nm) intensity as a function of time for the reaction between $[Co((\pm)\text{-bamap})H_2O]^+$ and Fe((*S*,*S*)-alamp). The sign of the CD signal corresponds to $\Lambda\text{-}(-)_{436}\text{-}[Co((S,S)\text{-bamap})(H_2O)]^+$, which must, therefore, be the enantiomer with the smaller reaction rate.

From the known CD and VIS spectra of the optically pure compounds, the relative concentrations of both antipodes can be obtained separately as a function of time. The corresponding first-order rate plot is given in *Fig. 5b*. In this representation, the net stereoselectivity of the reaction appears clearly.

If the reaction is followed by measuring the intensity of the CD signal at constant wavelength ($\lambda = 365$ nm), an interesting observation is made. At low concentrations of ascorbic acid ($c < 0.02$M), the CD signal does not return to a value near zero at the end of the reaction, but reaches a final and constant value, which depends on the amount of ascorbic acid present as well as on the concentrations of Fe(II) and (*S*,*S*)-alamp. The CD spectra of the final solution corresponds to the spectrum of $[Co((S,S)\text{-alamp})H_2O]^+$, indicating that a certain amount of this compound has been formed during the reaction, corresponding to an apparent ligand exchange following *Eqn. 3:*

$$[Co^{III}(bamap)(H_2O)]^+ + L^{2-} \xrightarrow{Fe(II)L} Co^{III}L^+ + bamap^{2-} \qquad (3)$$

This apparent ligand exchange must be brought about by the action of the Fe(III)/Fe(II) couple, no reaction is observed between $[Co((\pm)\text{-bamap})(H_2O)]^+$ and Co^{2+} in the presence of (*S*,*S*)-alamp during the time-scale used. The redox-mediated formation of $[Co((S,S)\text{-alamp})(H_2O)]^+$ may, therefore, be explained by the following reaction sequence:

$$[Co^{III}(bamap)]^+ + Fe^{II}L \rightarrow Fe^{III}L^+ + Co^{II}(bamap) \qquad (4)$$

$$Fe^{III}L^+ + Co^{II}(bamap) \rightleftharpoons Fe^{III}(bamap)^+ + Co^{II}L \qquad (5)$$

$$[Co^{II}L] + \begin{Bmatrix} [Fe^{III}L]^+ \\ [Fe^{III}(bamap)]^+ \end{Bmatrix} \rightarrow [Co^{III}L]^+ + \begin{Bmatrix} [Fe^{II}L] \\ [Fe^{II}(bamap)] \end{Bmatrix} \qquad (6)$$

ascorbic acid

L = $alamp^{2-}$

The Co^{II}, Fe^{II}, and Fe^{III} species are labile, the amount of the different complexes are under the control of the corresponding equilibrium constants, and the free metal ions may, therefore, also interfere in the reaction sequence too.

The amount of optically active Co(III) complex formed depends on the concentration of ascorbic acid because of the competition in the reduction of the Fe^{III}-species by the Co^{II} complexes and the ascorbic acid. At the end of the reaction, all the iron present is in the Fe^{2+} form and the amount of $[Co((S,S)\text{-alamp})(H_2O)]^+$ remains constant, indicating that this compound is not reduced by Fe^{2+} under the prevailing conditions. A detailed study of this reaction will be published in a following paper.

When $[Co((\pm)\text{-bamap})(H_2O)]^+$ reacts with Fe^{2+} in the presence of (*S*,*S*)-valmp, the third ligand described in this work, only a small stereoselectivity effect is observed, and

Table 2. *Stereoselectivity in the Electron Transfer between [Co(bamap)H_2O]$^+$ and Optically Active FeL Complexes*

L	pH	*Method*[a])	$k_{\Delta\Delta}/k_{\Lambda\Lambda}$[b])	$\Delta\Delta G^{\neq}$ (kJ·M^{-1})
bamap	3.5	*a*	1	0
alamp	4.0	*a*	1.7	1.3
	4.0	*b*	1.9	1.6
valmp	4.0	*b*	1.2	0.45

[a]) *a)* Variation of ee during the reaction from CD measurements; *b)* kineties of two diastereoisomeric couples.
[b]) Mean values of at least five runs; for reaction conditions, see *Fig. 5*.

the formation of [Co((*S,S*)-valmp)(H_2O)]$^+$ is even more important than in the case of (*S,S*)-alamp. For these reasons, the stereoselectivity of the reaction was determined by separate measurements of the reaction between both enantiomers of the optically active Co(III) complexes and [Fe((*S,S*)-valmp)]. The results obtained for the three optically active ligands are reported in *Table 2*.

3. Discussion. – When [Co(bamap)(H_2O)]$^+$ reacts with aqua-Fe^{2+}, two reaction paths can be observed: one pH-independent and the other pH-dependent. For the latter, two different intermediates can theoretically exist (*Eqns. 7* and *8*).

$$LCo{-}OH + Fe^{2+} \rightleftharpoons LCo{-}\underset{\displaystyle H}{O}{-}Fe^{2+} \rightarrow CoL + FeOH^{2+} \qquad (7)$$

$$LCo{-}OH_2^{+} + FeOH^{+} \rightleftharpoons LCo{-}\underset{\displaystyle H}{\overset{\displaystyle H}{O}}{-}FeOH^{2+} \rightarrow CoL + FeOH^{2+} \qquad (8)$$

A distinction between these two possibilities can be achieved by the effect of ionic strength on the reaction rate. Whereas in *Eqn. 7* the charge product of the reacting species is zero, it is +1 in *Eqn. 8*. Reaction rate should, therefore, be independent of the ionic strength in the former case, but increase with increasing ionic strength in the latter. In a range from 0.1 to 0.5, the corresponding measurements showed no influence of ionic strength on the reaction rate, indicating that the reaction proceeds by the OH^--bridged intermediate. This seems reasonable by the fact that the OH^- ion is known to be a much better bridging group than H_2O, also for electrostatic reasons.

Assuming the proposed mechanism, it is seen from the obtained data, that [Co(bamap)(OH)] reacts about $1.3 \cdot 10^4$ times faster with the aqua-Fe^{2+} than [Co(bamap)(H_2O)]$^+$.

The question on the reaction mechanism between the two aqua complexes then arises. The H_2O molecule being, if at all, considered as a weak bridging group, it may be inferred that the reaction should be of the outer-sphere type, or that the bridging of the two metal centers take place by an other group, *e.g.* one of the coordinated COO groups.

On the other hand, the observed stereoselectivity in the overall electron-transfer reaction with the optically active Fe^{2+} complexes implies a rather close approach of the two chiral faces of the reacting complexes. From X-ray data [16] and from model considerations, it is possible to estimate the distances between the two metal centers at which steric interactions between the Me groups of the [Co(bamap)] moiety and the substituents of the optically active Fe^{2+} complexes begin to occur, when the coordination sphere of one metal center of the binuclear intermediate is rotated around the Co-X-Fe

axis. It follows that neither an outer-sphere mechanism nor bridging by a COO group can explain the observed relative stereoselectivities, and we conclude, therefore, that the reaction takes place by an inner-sphere mechanism through a H_2O-bridged binuclear transition state *(Fig. 6)*.

As a further argument for the proposed mechanism, it may be mentioned that the reaction between [Co(bamap)Cl] and Fe(alamp) shows a higher reaction rate, due to the better bridging ability of Cl^-, and a stereoselectivity with the same geometrical orientation and the same order of magnitude as the aquo-complex, indicating that the reaction takes place by a similar mechanism [17].

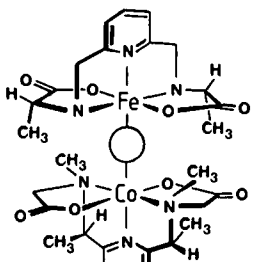

Fig. 6. *Proposed structure of binuclear transition state in the reaction between Δ-[Co((R,R)-bamap)(H_2O)]$^+$ and Λ-[Fe((S,S)-alamp)]*

From *Fig. 6*, it can be recognized that the chiral faces of the two reacting complexes fit better, when they exhibit opposite chirality. In all the reactions of [Co(bamap)(H_2O)]$^+$ or [Co(bamap)Cl] studied so far with the different Fe^{2+} complexes described in this paper, and for which stereoselectivity could be observed, the *Δ-Λ* couple reacts faster than the *Δ-Δ* or *Λ-Λ* couple, in accordance with the model.

When the second-order rate constants of the electron transfer between [Co(bamap)-(H_2O)]$^+$ and the aqua-Fe^{2+} are compared with the analogous reactions involving the different Fe^{2+} complexes, a 10^4 to 10^5 fold increase is observed. This acceleration can be a consequence of the reduction of the positive charge of the reducing agent as well as a reduction of the *Franck-Condon* rearrangement term, which contributes to the free activation energy.

On the other hand, it can not been decided, if the reaction involves the formation of a precursor complex, and whether the observed stereoselectivity is a consequence of a difference in the stability of the precursor complex or of the rate of the intramolecular electron transfer following the formation of the binuclear precursor.

Experimental Part

1. *General.* Optical rotations were measured on a *Perkin-Elmer 241* polarimeter, UV and VIS spectra on a *Uvikon 820* spectrophotometer, and CD measurements were obtained from a *JASCO J-500* spectropolarimeter. ^{1}H-NMR: recorded on a *Bruker WP 200* at 200 MHz.

2. *Syntheses.* 2.1. *Aqua[2,6-bis(3-carboxy-1,2-dimethyl-2-azapropyl)pyridine]cobalt(III) Perchlorate* ([Co(bamap)H_2O][ClO_4]·2 H_2O). The racemic and the two optically active complexes were prepared as described in [1] and isolated as perchlorate salts by crystallization from 10% aq. $NaClO_4$.

2.2. *2,6-Bis[(3R,3S)-3-carboxy-1,2-dimethyl-2-azapropyl]pyridine* ((*R,S*)-bamap). When bamap is prepared as described in [1], a mixture of the *meso* and the racemic isomer, which could be separated only as their Co(III)

complexes, is obtained. The pure racemic ligand was, therefore, obtained by decomposition of the corresponding Co(III) complex: *rac*-[Co(bamap)(H_2O)][ClO_4]·2 H_2O (1 g, 1.92 mmol) is heated to 50° with KCN (1.3 g, 20 mmol) in 50 ml of H_2O during 6 h. H_2O_2 (1 ml; 30%) is then added to the yellow soln., and the temp. maintained at 50°. After 1 h, AcOH (5 ml) is added and the free HCN eliminated in the hood by bubbling a stream of air through the warm soln. under slightly reduced pressure. After cooling, the soln. is introduced into a small cation-exchange column *(Dowex 50, H^+)*, and the hexacyanocobaltate and other products washed out with H_2O. Elution with 0.2N NaOH and evaporation to dryness of the neutral fractions containing the ligand yields *rac*-H_2bamap as a colourless oil. All attempts to crystallize the product failed. It was characterized by potentiometric titration and the NMR spectrum, which is very similar to the one obtained for the mixture of the two diastereoisomeres [1]. ^{1}H-NMR (D_2O): 1.7 (*d*, 6 H); 3.0 (*s*, 6 H); 3.6 (*s*, 4 H); 4.8–4.9 (*m* unresolved, 2 H); 7.6 (*d*, 2 H); 8.1 (*t*, 1 H).

2.3. *2,6-Bis[(3S)-3-carboxy-1,2-dimethyl-2-azapropyl]pyridine* ((*S,S*)-bamap). The compound was isolated by the procedure indicated under *2.2* from (−)$_{436}$-[Co(bamap)(H_2O)][ClO_4]·2 H_2O ([α](λ) = −1000° (436)). As for the racemic product, the optically active ligand could not be obtained in a crystalline form. [α](λ): −185° (436); −82° (589) (*c* = 0.46, H_2O, pH 4).

2.4. *2,6-Bis[(3S)-3-carboxy-2-azabutyl]pyridine* ((*S,S*)-alamp). Sodium (*S*)-alaninate (10.1 g, 0.1 mol), obtained by neutralization of (*S*)-alanin with a stoichiometric amount of NaOH, dissolved in MeOH (30 ml), is introduced in a 250-ml flask and heated to 50°. 2,6-Bis(bromomethyl)pyridine (5.4 g, 20 mmol) dissolved in MeOH (150 ml) is slowly added under stirring. After complete addition, the mixture is heated to 60° during 6 h, and the pH is kept constant at 9.6 by addition of NaOH/MeOH. After cooling, 2.13 g of unreacted alanin are filtered off and the filtrate is evaporated to dryness. The residue is redissolved in H_2O and the soln. is introduced in a cation-exchange column *(Dowex 50 X-8, H^+)*. The column is washed to neutrality with H_2O and the product eluted with 0.1M NaOH. Unreacted (*S*)-alanine is eluted first followed by a fraction containing a mixture of (*S*)-alanine and (*S,S*)-alamp. The effluent is analyzed by TLC (silica gel; BuOH/AcOH/H_2O 12:6:5) and by UV and polarimetric measurements. The fraction containing the (*S,S*)-alamp is evaporated to dryness and the residue washed with MeOH. After repeated recrystallization from H_2O/EtOH or H_2O/acetone, 2.25 g (39%) of the product, showing no more trace of alanine by TLC, is obtained. F 265°, [α]$^{r.t.}$(λ): +45.2° (365), +26.1° (436) (*c* = 0.26, H_2O). ^{1}H-NMR (D_2O, 200 MHz): 1.68 (*d*, 6 H); 3.80 (*q*, 2 H); 4.46 (*s*, 4 H); 7.47 (*d*, 2 H); 7.94 (*t*, 1 H). Anal. calc. for $C_{13}H_{19}N_3O_4$ (281.3): C 55.51, H 6.81, N 14.94; found: C 55.07, H 6.73, N 14.69.

2.5. *2,6-Bis[(3R)-3-carboxy-2-azabutyl]pyridine* ((*R,R*)-alamp). Prepared as the (*S,S*)-enantiomer. 2,6-Bis-(bromomethyl)pyridine (77.6 g, 0.7 mol) and sodium (*R*)-alaninate (60.1 g, 0.227 mol) gave 17.3 g (27.1%) of the pure product, after separation and crystallization. [α]$^{r.t.}$(λ): −47.9° (365), −26.9° (436) (*c* = 0.2, H_2O).

2.6. *2,6-Bis[(3S)-3-carboxy-4-methyl-2-azapentyl]pyridine* ((*S,S*)-valmp). The procedure from [1] was modified as follows: 2,6-bis(bromomethyl)pyridine (10 g, 0.038 mol) in MeOH (150 ml) is added slowly to a vigorously stirred soln. of sodium (*S*)-valinate (27.5 g, 0.198 mol) in MeOH (50 ml). During the addition, a certain amount of valine precipitates. A methanolic soln. of 1.5 g of NaOH is added in order to maintain the pH of the mixture at 10–11. After 7 h, at 60°, the mixture is cooled, filtered, and the filtrate evaporated to dryness. The residue is redissolved in H_2O, and the (*S,S*)-valmp is purified on *Dowex 50* (H^+) and isolated in the same manner as indicated in *2.4* for (*S,S*)-alamp. After five recrystallizations from H_2O/acetone, 4.3 g (34%) of the pure product is obtained. [α]$^{r.t.}$(λ): +19.4° (365), +11.9° (436), +5.4° (589) (*c* = 0.45, H_2O). ^{1}H-NMR (D_2O, 200 MHz): 1.07 (*t*, 12 H); 2.32 (*m*, 2 H); 3.55 (*d*, 2 H); 4.45 (*s*, 4 H); 7.5 (*d*, 2 H); 7.96 (*t*, 1 H). Anal. calc. for $C_{17}H_{27}N_3O_4$ (337.4): C 60.51, H 8.07, N 12.45; found: C 60.43, H 8.08, N 12.40.

2.7. *2,6-Bis[(S)-(2-carboxypyrrolidin-1-yl)methyl]pyridine* ((*S,S*)-promp). Synthesized in a way similar to that described in *2.4*, by reacting sodium (*S*)-prolinate (25 g, 0.182 mol) with 2,6-bis(bromomethyl)pyridine (10 g, 0.038 mol). When the reaction mixture is fixed on *Dowex 50* (H^+), the unreacted proline can be eluted with H_2O. The column is washed with H_2O, as long as the effluent shows any optical activity. The (*S,S*)-promp, which is then eluted with 0.1M NaOH, could not be obtained in a crystalline form. The neutral soln. containing the product, identified by its UV absorption and its optical activity, was, therefore, directly used without further purification for the synthesis of the Co(III) complex.

2.8. *Pyridino(2,6-bis[(3S)-3-carboxy-2-azabutyl]pyridine)cobalt(III) Perchlorate* ([Co((*S,S*)-alamp)(py)]-[ClO_4]·H_2O). (*S,S*)-alamp (0.158 g, 0.562 mmol) is added to [Co(py)$_4$Cl$_2$]Cl dissolved in H_2O (50 ml). By heating to 40–50° during several min, the soln. turns from green to red. After 2 h, the soln. is introduced into a cation-exchange column (*Sephadex SP C25*, Na^+) which fixes the complex quantitatively. Elution with 0.2% $NaClO_4$ yields two orange-red bands, the second containing a small quantity of the aqua-complex. Concentration of the soln. containing the main band yields the perchlorate salt of the mixed complex with a coordinated pyridine. The red crystals are filtered and recrystallized from H_2O. ^{1}H-NMR (DMSO, 200 MHz): 0.67 (*d*, 6 CH_3); 3.43 (unresolved, 2 CH); 4.63 (*d*, CH_2); 5.1 (*q*, CH_2); 7.53 (*d*, 2 NH, exchange with D_2O); 7.75, 7.94, 8.3, 8.9 (8 arom. H).

Anal. calc. for $[Co(C_{13}H_{17}N_3O_4)C_5H_5N][ClO_4]\cdot H_2O$ (535): C 40.40, H 4.53, N 10.48; found: C 40.26, H 4.35, N 10.64.

2.9. *Pyridino(2,6-bis[(3S)-3-carboxy-4-methyl-2-azopentyl]pyridine)cobalt(III) Hexafluorophosphate* ([Co((*S,S*)-valmp)(py)][PF_6]). (*S,S*)-valmp (0.95 g, 2.7 mmol) is added to a soln. of $[Co(py)_4Cl_2]Cl$ (1.3 g, 2.7 mmol) in H_2O. On standing at r.t., the colour of the soln. rapidly turns to red. After heating to 30–40° during 1 h, the soln. is introduced into a cation-exchange column (*Sephadex SP C25*, Na^+). Elution of the complex, which is quantitatively fixed on the column with 0.1% NaCl, yields a single band. UV and CD of samples from the head and the end of the band were perfectly identical, showing that a single compound is formed in the reaction. The soln. containing the product is concentrated, and the hexafluorophosphate is precipitated as a yellow-orange crystalline powder by addition of NH_4PF_6. Recrystallized from H_2O. $[\alpha]^{r.t.}(\lambda)$: −1037° (436), −540° (546), −370° (589) ($c = 0.1$, H_2O). ^{1}H-NMR (DMSO, 200 MHz): 0.08 (*d*, 2 CH_3); 0.88 (*d*, 2 CH_3); 1.97 (*m*, 2 $(CH_3)_2CH$); 3.24 (unresolved, $CHCH(CH_3)_2$); 4.4 (*d*); 6.94 (*s*, 2 NH, exchange with D_2O); 7.85, 8.25, 8.93 (3*m*, 8 arom. H). Anal. calc. for $[Co(C_{17}H_{25}N_3O_4)C_{15}H_5N][PF_6]$ (618): C 42.58, H 4.88, N 9.03; found: C 40.81, H 5.08, N 8.66.

2.10. *Pyridino(2,6-bis[(S)-(2-carboxypyrrolidin-1-yl)methyl)pyridine]cobalt(III) Perchlorate* ([Co((*S*)-promp)(py)][ClO_4]). One (theoretical) equiv. of $[Co(py)_4Cl_2]Cl$ (18.3 g) is added to the soln. of (*S,S*)-promp obtained as described in *2.7*. The mixture is heated to 40° during 1 h, filtered, and introduced into a cation-exchange column (*Sephadex SP C25*, Na^+) and thorougly washed with H_2O. On elution with 0.1% NaCl, several bands develop. The red coloured main fraction is concentrated, and after elimination of NaCl by elution on *Sephadex G10*, the product is purified by a second chromatographic elution with 0.2% $NaClO_4$ on the cation-exchange column. Concentration of the effluent yields 8.5 g (47%) of red crystals of the perchlorate salt. Recrystallized twice from H_2O. $[\alpha]^{r.t.}(\lambda)$: −1000° (436), +35° (546), −385° (589) ($c = 0.1$, H_2O). ^{1}H-NMR (NO_3^- salt in D_2O, 200 MHz): 0.4 (*m*, CH_2 of pyrrolidine); 1.85 (*m*, 2 CH_2 of pyrrolidine); 2.4 (*m*, CH_2 of pyrrolidine); 3.28 (*m*, CH_2 of pyrrolidine); 3.9 (*q*, H–C(2) of pyrrolidine); 4.64 (*d*, CH_2); 5.15 (*d*, CH_2); 7.95, 8.4, 8.8 (3*m*, 8 arom. H). Anal. calc. for $[Co(C_{17}H_{21}N_3O_4)C_5H_5N][ClO_4]$ (569): C 46.45, H 4.16, N 9.85; found: C 46.27, H 4.52, N 9.99.

3. *Solutions.* All the reagents used were of anal. grade. Solns. for kinetic measurements were prepared under N_2, and a N_2 atmosphere was maintained during the reactions. Solns. of Fe(II) salt and ascorbic acid were freshly prepared each day. The reaction temp. was controlled within 0.1°.

The authors wish to thank Dr. *C. Saturnin* for the measurements and discussion of NMR spectra and *Ch. Scheuermann* and *N. Vantaggio* for the execution of part of the measurements.

REFERENCES

[1] K. Bernauer, P. Pousaz, *Helv. Chim. Acta* **1984,** *67,* 796.
[2] P. Osvath, A. G. Lappin, *Inorg. Chem.* **1987,** *26,* 195.
[3] P. Osvath, A. G. Lappin, *J. Chem. Soc., Chem. Commun.* **1986,** 1056.
[4] D. P. Martone, P. Osvath, Ch. Eigenbrot, M. C. M. Laranjeira, R. D. Peacock, A. G. Lappin, *Inorg. Chem.* **1985,** *24,* 4693.
[5] D. A. Geselowitz, H. Taube, *J. Am. Chem. Soc.* **1980,** *102,* 4525.
[6] B. Pispisa, R. Rizzo, G. Paradossi, *J. Inorg. Biochem.* **1986,** *26,* 281.
[7] B. Pispisa, M. Barteri, M. Farinella, *Inorg. Chem.* **1983,** *22,* 3166.
[8] S. Sakaki, T. Satoh, K. Ohkubo, *New J. Chem. (CNRS-Gauthier Villars)* **1986,** *10,* 145.
[9] A. G. Lappin, M. C. M. Laranjeira, R. D. Peacock, *Inorg. Chem.* **1983,** *22,* 786.
[10] S. Kondo, Y. Sasaki, K. Saito, *Inorg. Chem.* **1981,** *20,* 429.
[11] I. I. Creaser, A. M. Sargeson, A. W. Zanella, *Inorg. Chem.* **1983,** *22,* 4022.
[12] Y. Sasaki, K. Meguro, K. Saito, *Inorg. Chem.* **1986,** *25,* 2277.
[13] Y. Kaizu, T. Mori, H. Kobayashi, *J. Phys. Chem.* **1985,** *89,* 322.
[14] D. A. Geselowitz, A. Hammershoi, H. Taube, *Inorg. Chem.* **1987,** *26,* 1842.
[15] Ph. Benson, A. Haim. *J. Am. Chem. Soc.* **1965,** *87,* 3826.
[16] H. Stoeckli-Evans, L. Brehm, Ph. Pousaz, K. Bernauer, H.-B. Bürgi, *Helv. Chim. Acta* **1985,** *68,* 185.
[17] K. Bernauer et al., to be published.
[18] B. E. Leach, R. J. Angelici, *J. Am. Chem. Soc.* **1969,** *91,* 6296.
[19] R. Nakon, P. R. Rechani, R. J. Angelici, *Inorg. Chem.* **1973,** *12,* 2431.

Liste des publications :

1. K. Bernauer, Ph. Pousaz, Helv. Chim. Acta, *1984*, 67, 796

2. H. Stoeckli-Evans, L. Brehm, Ph. Pousaz, K. Bernauer, H.-B. Bürgy, Helv. Chim. Acta, *1985*, 68, 185

3. K. Bernauer, Ph. Pousaz, Helv. Chim. Acta, *1988*, 71, 1339

Note : le texte complet de la thèse est déposé à la bibliothèque de l'Université de Neuchâtel